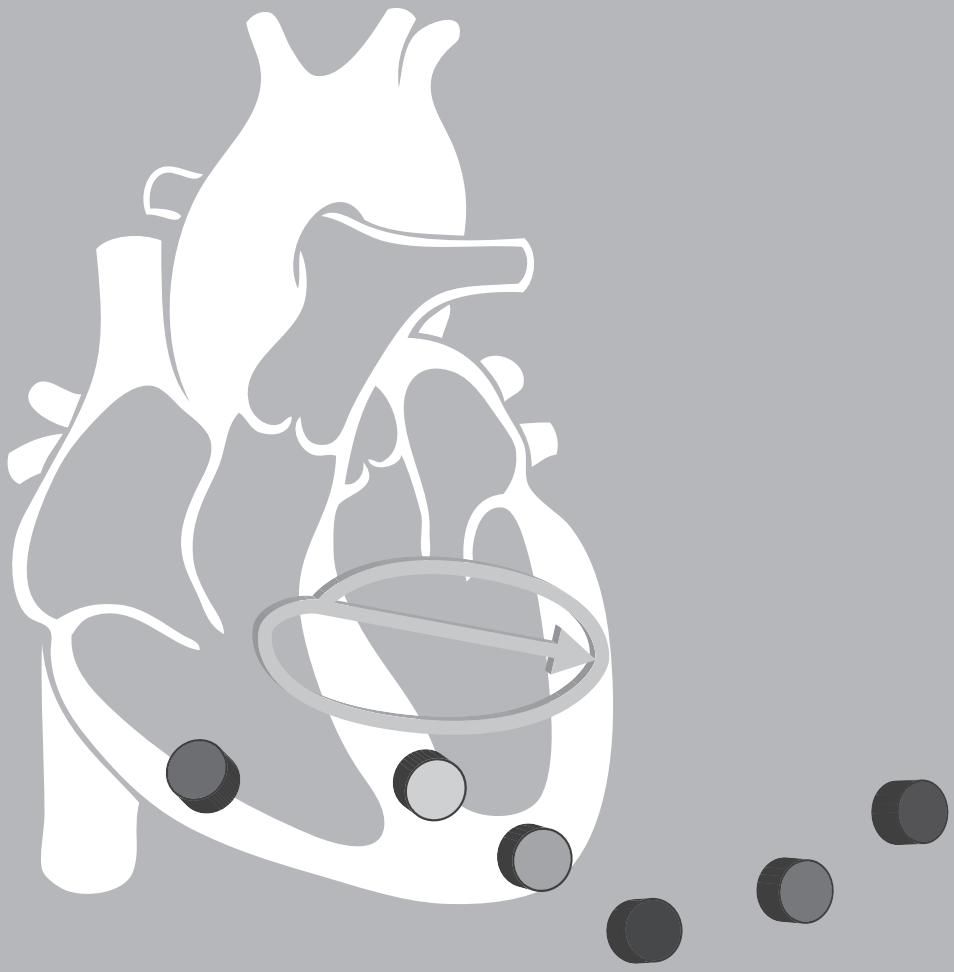

Chapter 1

General introduction
Adapted from "Vectorcardiographic diagnostic & prognostic information derived from the 12-lead electrocardiogram: historical review and clinical perspective"

Sum-Che Man, Arie C. Maan, Martin J. Schalij, Cees A. Swenne

J Electrocardiol 2015; 48: 463-475

Background

Since cardiology emerged from internal medicine as a distinct medical specialty[1], various modern technologies have been prominently present in its diagnostic and interventional/therapeutic procedures. One of these was the (surface) electrocardiogram (ECG) that has not subsided since its introduction more than a century ago, and is nowadays present in many forms with a plethora of electrode configurations and recording durations in settings varying from resting conditions to dynamic situations[2]. When tracing back the development of electrocardiology from its initial primitive form at the end of the nineteenth century (the first human electrocardiogram was published by Waller in 1887[3]) to its current form in the beginning of the twenty-first century, tens of seminal contributions by scientists, engineers and physicians can be mentioned[4;5].

The vectorcardiogram (VCG) is a special form of ECG. In this Chapter, we discuss the origins and essentials of the VCG and how this emerged in the 1950's and 60's partly replacing the standard 12-lead ECG. We also discuss the temporary decrease in the interest in vectorcardiography in the 1970's and 80's, and the revival of vectorcardiography in the 90's, when it became increasingly popular to mathematically synthesize a VCG from a standard 12-lead ECG, eliminating the need for dedicated VCG recording equipment. Finally, we discuss the potential future incorporation of VCG-derived information in routine clinical 12-lead electrocardiography.

Origin of the electrocardiogram

The information content of any particular form of electrocardiography obviously depends on the electrode configuration (number and positions of the electrodes utilized to sample the body surface potential distribution in space and time). Current electrocardiography relies in large part on signals derived from 9 electrodes; 3 extremity electrodes at the left arm (LA), right arm (RA) and left foot (LF), as already used by Einthoven[6;7], and 6 chest electrodes (C1-C6) of which of the positions were standardized in 1938[8-10]. The twelve leads as we are using them today have been introduced by Einthoven (who derived extremity leads I, II, and III from the LA, RA and LF electrodes[6;7]), Goldberger (who derived the augmented extremity leads aVR, aVL, and aVF from the same electrodes[11]), and Wilson *et al.* (who contributed

to the derivation of the precordial leads V1-V6 from chest electrodes C1-C6 by introducing the "central terminal", *i.e.*, the average of the LA, RA and LF extremity electrode potentials[12]). To do justice to history, chest electrodes had been used earlier, however in combination with an electrode on the back, by Waller[3] and Wolferth *et al.*[13].

In fact, the term 12-lead ECG is slightly confusing, because nine electrodes can produce only eight independent leads. As the six extremity leads I, II, III, aVR, aVL and aVF are all derived from three electrodes, only two extremity leads carry independent information, the other four are completely redundant. Usually, leads I and II are selected to represent the six extremity leads. Hence, extremity leads I and II, and chest leads V1-V6 contain all information obtained with electrodes LA, RA, LF and C1-C6. A variant of the standard 12-lead ECG is recorded with the extremity electrodes placed on the torso just proximal to the right arm, left arm and left leg (Mason-Likar electrode configuration[14]). This variant 12-lead ECG, of which the information content is slightly different from the standard 12-lead ECG[15], is typically used in situations where distal extremity electrodes at wrists and ankle would likely cause noise (*e.g.*, in the setting of exercise) or where distal extremity electrodes would be inconvenient (*e.g.,* in the setting of emergency and/or monitoring).

Heart vector and lead vector

Another, parallel line of development in electrocardiography relates to the vector concept. In the first articles concerning the human electrocardiogram[16;17], Augustus D. Waller pointed out the dipolar nature of the cardiac electric generator on the basis of a body surface isopotential map, see Figure 1. Because it is possible to describe the electric generator of the heart reasonably accurately with an equivalent dipole, it is natural to display it in vector form[18] (in physics, an electrical dipole is denoted as a vector, depicted as an arrow with given orientation and length, representing the direction and strength of the dipole, respectively). Einthoven already displayed the electrical activity of the heart in the form of an arrow ("Pfeil"), on the shaft of which a segment *pq* was chosen to represent the momentary potential difference *E* that was projected on the three sides of an

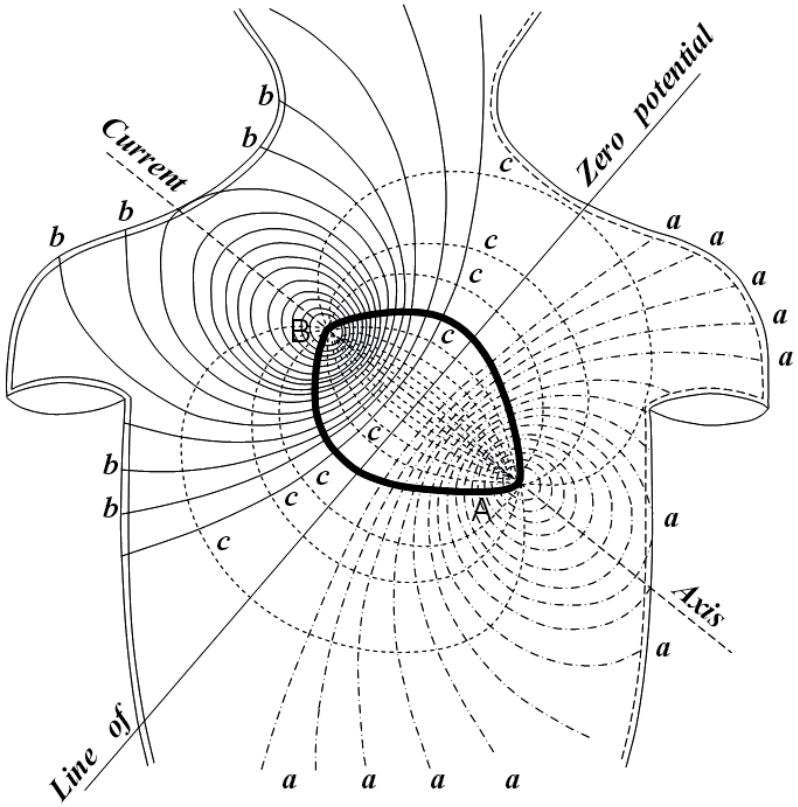

FIGURE 1. Body surface isopotential map; modified[18] from Waller[17], with permission. This isopotential and current flow lines as reconstructed by Waller demonstrate the dipolar nature of the cardiac electrical activity. A: point of the most positive potential, the localization of which is assumed to correspond to the intracavitary position of the apex of the heart; B: point of the most negative potential, corresponding to the base of the heart; a: isopotential lines, positive potentials; b: isopotential lines, negative potentials; c: current flow lines.

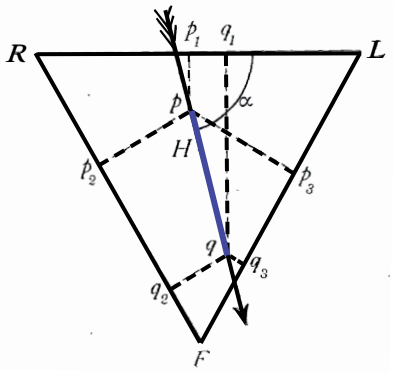

FIGURE 2. Vector representation of the electrical activity of the heart at a given moment; Figure 22 from Einthoven[7], with permission. Actually, the vector magnitude equals the segment pq (we marked this in Einthoven's original figure by a blue line) on the shaft of the arrow, and not the length of the entire arrow. Vector projection on the three sides of the equilateral "Einthoven" triangle yield the amplitudes p_1q_1, p_2q_2, p_3q_3 in leads I, II, and III, respectively.

equilateral triangle, thus resulting in potential differences e_1, e_2, and e_3 in leads I, II, and III, respectively[6;7], see Figure 2.

An essential step forward was made by Burger[19] and coworkers who laid the theoretical background for vectorcardiography and conceived — based on thorough mathematical and physical knowledge and ample experimentation with a phantom model — the notions of heart vector, lead vector and image space[20;21]. In short, the heart vector represents the momentary total cardiac electrical dipole strength and direction. The momentary amplitudes of the voltages in the various electrocardiographic leads are determined by projecting the heart vector on the lead vectors associated with each electrocardiographic lead, and multiplying these projections by the lead-vector magnitudes (strengths), see Figure 3 for explanation. For a given heart vector $\vec{H}$ and a given ECG lead with lead vector $\vec{c}$, Burgers equation for the voltage in that lead, *V*, reads

$$V = \vec{c} \cdot \vec{H} \qquad \text{(Eq. 1)}$$

Direction and strength of a particular lead vector depend on the distances of the involved electrodes to the heart and the inhomogeneity of the conductive properties in the thorax. These properties represent the direction in which the particular lead "sees" the heart vector, and the sensitivity of this lead, respectively. Thus, lead vectors take the distortions caused by the boundary and internal inhomogeneities of the body into account. The lead vector concept is a major improvement from the common oversimplified interpretation in which it is assumed that the spatial direction of the line connecting an electrode pair determines the orientation of the lead. It is essential to realize that a particular ECG lead "sees" the heart vector from a different direction and with a different sensitivity as what would be expected on the basis of the positions of the electrodes associated with that lead. Burger, realizing that lead vectors mapped the heart vector into a space different from physical space, termed this "image space" in a seminal 1948 publication[20]. At the same time as the image space was introduced, he described that this would facilitate to inversely reconstruct the heart vector from the ECG.

The difference between Einthoven's and Burger's approaches is dramatic, as becomes immediately clear when comparing Einthoven's equilateral triangle

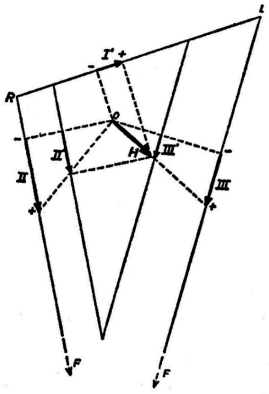

FIGURE 3. Burger's scalene triangle; Figure 37 from Boutkan[22], with permission. Analogous to Einthoven, Burger made this triangle projection representation to illustrate the consequences of the lead vector concept for Einthoven's theory. In Burger's triangle, the lengths of the sides (inner triangle with closed corners) represent the lead strength (sensitivity), and the direction of the sides represent the direction in which the leads "see" the heart vector (H). Comparing the Burger and Einthoven triangles reveals two basic differences. First, the directions in which the leads see the heart vector are not neatly 60° different: lead I assumes a slight upward direction, and leads II and III make a very sharp angle (and appear, compared to Einthoven, to be more in the same direction). Secondly, there is a remarkable difference in the sensitivities of the leads, lead I being least sensitive, lead III having the highest sensitivity. The difference in the lead vector directions (the directions of the sides of the inner triangle) cause a different projection of the heart vector on the inner triangle (compare with Einthoven's projection in Figure 2). Moreover, after projection, the resulting vectors have to be multiplied by the strength of the leads (the relative length of the sides of the inner triangle). Arbitrarily taking, in this graphical representation, the strength of lead vector I as reference, the voltage in this lead, I', is straightforwardly found by the projection of the heart vector H on that lead vector. Leads II and III have larger strengths (longer sides of the inner triangle). Hence, the projections of the heart vector on the lead vectors II and III (II' and III', respectively) have to be amplified by the relative strength of these lead vectors with respect to the strength of lead vector I to find the voltages in these leads (II and III, respectively). These multiplications have graphically been realized in this Figure by the help of an extra outer triangle with sides parallel to the inner triangle at appropriate distances.

projection (Figure 2) with Burger's scalene triangle projection with correction for lead strengths (Figure 3). *E.g.*, Einthoven's lead vector I has a horizontal direction and its strength equals the lead II and lead III strengths, whereas Burger's more correct lead vector I inclines about 17° and its strength is considerably smaller than that of leads II and III[23].

More complex modelling approaches of the electrical source of the ECG (moving instead of fixed dipole, multiple dipole and multipole[24]) have never gained popularity, and the above described theoretical basis of electrocardiography (equivalent dipole at a fixed location, heart vector, lead vector) is considered a valid approach today. In clinical practice, these relevant physical considerations are often neglected, however: ECG interpretation is still done in Einthoven's physical space. *E.g.*, several clinical textbooks postulate that the extremity leads are purely in the frontal plane and the chest leads are purely in the transverse plane; moreover, the angles between the lead vectors in the frontal plane are supposed to be multiples of 30°. Figure 4 shows that these assumptions are far from correct, and

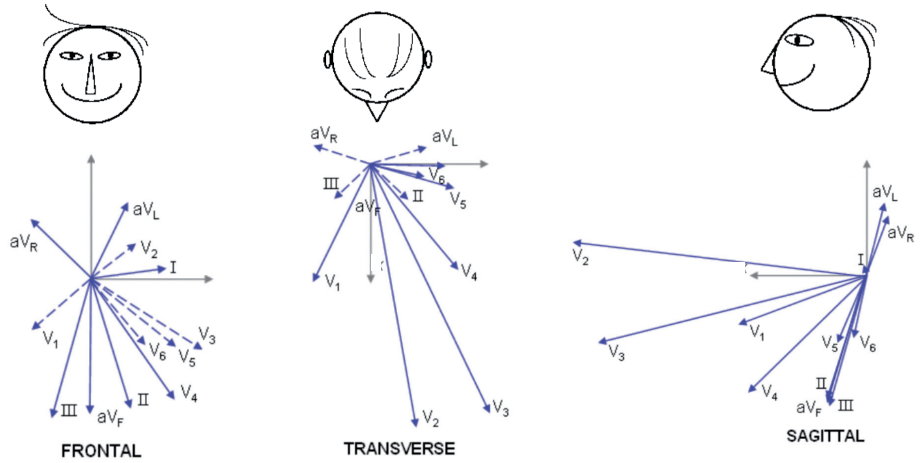

FIGURE 4. Lead vectors of the 12-lead ECG; modified after Figure 18.1 from Bioelectromagnetism[25] , with permission. Components of the extremity lead vectors I, II, III, aV_R, aV_L and aV_F that are generally assumed to be in the frontal plane are actually also in the transverse and sagittal planes. Components of the precordial lead vectors V1-V6 that are generally assumed to be in the transverse plane are actually also in the frontal and sagittal planes. Moreover, striking differences in lead strengths are seen. Also, the directions of the lead vectors differ sometimes dramatically from the idealized directions as usually depicted in text books (in the frontal plane aV_L, I, II, aV_F, III and aV_R at 2, 3, 5, 6, 7 and 10 o'clock, and in the transverse plane V6-V1 at 2-7 o'clock, respectively).

the irregular distribution of the directions and strengths of the lead vectors in the 12-lead ECG complicate straightforward ECG interpretation.

The vectorcardiogram

Accepting as model of the electrical activity of the heart a heart vector (the term vector was first used in this respect by Williams in 1914[26]) that represents the instantaneous dipole strength and direction, the major goal of electrocardiography would be the dynamic measurement of this heart vector. This would necessitate the recording of a vectorcardiogram (VCG), consisting of three orthonormal leads X, Y and Z, with lead vectors in the directions of the (orthogonal) main axes of the body and with equal (normalized) lead strengths, thus measuring the dynamic *x*, *y* and *z* components of the heart vector, respectively[23].

By combining the xy, xz, yz and xyz amplitudes, two-dimensional or three-dimensional patterns of movement of the heart vector, vector loops[18], can be constructed (see Figure 5) — the name "vectorcardiogram" was chosen by Wilson

and Johnston[27] in 1938; earlier, in 1936, Schellong[28] had introduced the word "vectordiagram" while Mann[29], who, in 1920, published the first vector loop, called it "monocardiogram". In contrast to scalar representations, these 2D and 3D Lissajous figures give insight into the time relationships between the leads, already mentioned by Williams in 1914[26]. It becomes immediately apparent from vector loops that the largest amplitudes in the leads are not reached at the same time. *E.g.*, in Figure 5, this can clearly be seen in the vector loops in the transverse and sagittal planes. In this example, the vector loop in the transverse plane shows that the largest amplitude in lead Z is attained well before the largest amplitude in lead X, and the vector loop in the sagittal plane shows that the largest amplitude

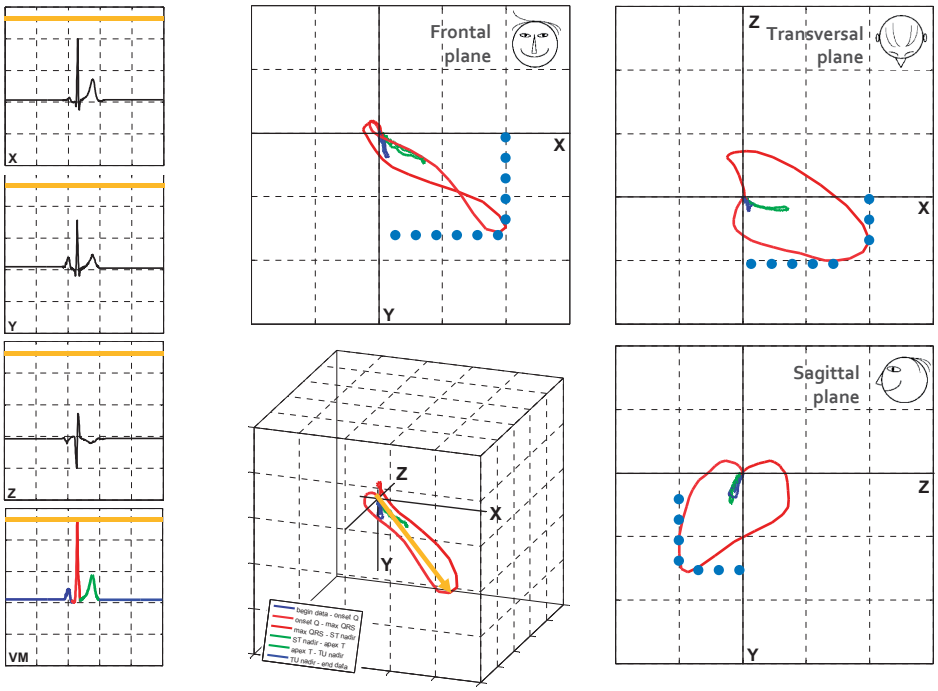

FIGURE 5. Scalar and Lissajous representations of the vectorcardiogram (VCG). Left panels, from top to bottom: scalar representations of the X, Y, and Z leads and of the vector magnitude (VM). Upper middle and right panels: 2D vector loops in the frontal, transverse and sagittal planes. Lower middle panel: 3D vector loop. Calibration: 0.5 mV/division. Colors mark the intervals between characteristic time instants in the ECG. Light red: onset QRS – instant of maximal QRS vector; dark red: instant of maximal QRS vector – end of QRS; light green: end of QRS – instant of maximal T vector; dark green: instant of maximal T vector – end of T; blue: ECG signal outside the QRS-T complex. The yellow arrow in the 3D vector loop indicates the maximal QRS vector. The magnitude of the maximal QRS vector is indicated in the 2D representations as a horizontal yellow line. The light blue-dotted lines in the 2D vector loops mark the lead-dependent maxima.

in lead Z is attained well before the largest amplitude in lead Y. Hence, the largest amplitude in the ECG is usually missed, because in general the direction of the heart vector at that very moment is not parallel to one of the lead vectors. The solution in vectorcardiography is to compute, as a fourth scalar lead, the vector magnitude according to the theorem of Pythagoras (root-sum-squared x-y-z amplitudes).

In the next decades, various systems for vectorcardiography were introduced, each with their own electrode configuration. The most known were those proposed by Burger *et al.*[21], McFee *et al.*[30], Schmitt *et al.*[31], and Frank[32]. Of these systems, the Frank system prevailed (see Figure 6). Due to important protagonists of the VCG like Robert P. Grant[33] (1915-1966) and J. Willis Hurst[34] (1920-2011), vectorcardiography was in routine clinical use in various hospitals in the 1960s, but the scalar

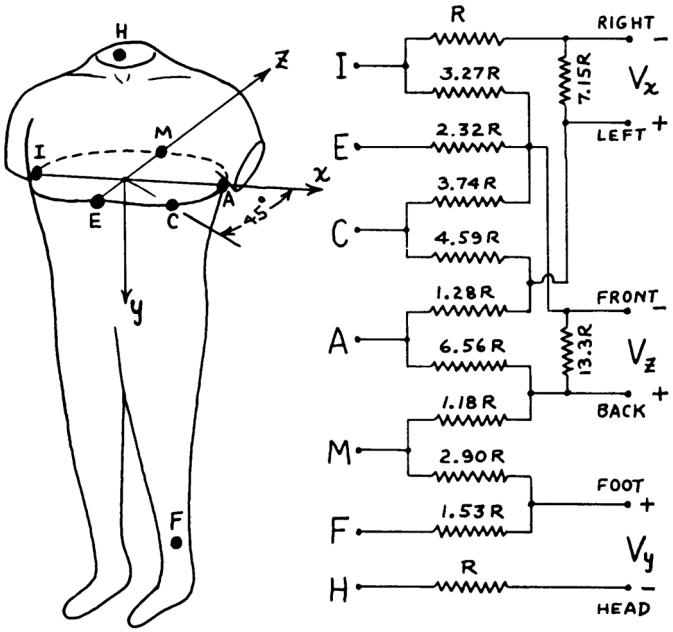

FIGURE 6. VCG lead system according to Frank[32], with permission. The 7 electrodes and the resistor network constitute a "corrected" lead system, i.e., lead vectors with equal strengths and pointing in the direction of the main axes of the body. The directions of the x, y and z-axes correspond to what later became the American Heart Association standard[36]. Each electrode contributes to each of the X, Y and Z leads, except for the "head" electrode that is exclusively used for the derivation of the Y lead. H= head; F = left foot; A, C, E, I and M are a selection of the electrodes that Frank used for an earlier study[37] where he placed electrodes all around the thorax in an anatomical transverse plane, designated in alphabetical order (A-P) and separated by 22.5° angles.

12-lead ECG, that had half a century of history as a clinical diagnostic tool[35] before the VCG was conceived, remained the most popular.

Decline of vectorcardiography

When both 12-lead electrocardiography and vectorcardiography were in clinical use, several studies appeared that compared ECG and VCG performance. Comparing 12-lead electrocardiography and vectorcardiography (*e.g.*, Frank system) can be done at the level of the information content of the signal, as well as at the level of the diagnostic algorithms[38]. Reasoning in terms of information content, the 12-lead ECG is measured by 9 electrodes (right leg reference electrode not included), which means that there are 9−1=8 independent leads. The Frank VCG is measured by 7 electrodes, of which 7−1=6 independent leads could be constructed. However, conceptually, the electrodes are combined in such a way that 3 leads (the supposedly orthonormal X, Y and Z leads) result. Apart from the question of which of these electrode configurations comprises the largest information content, it is obvious that the reduction in the number of leads in the VCG to 3 causes some information loss. It is therefore conceivable that, at the signal level, the 3 VCG leads X, Y and Z contain less information than the 8 ECG leads I, II, V1-V6. The advantages of the VCG are the orthonormality of the 3 leads and the availability of the phase relationships of these leads, which is a favorable basis for diagnostic algorithms that don't have access to such data in the 12-lead ECG. In this way, it is understandable that if adequately powerful diagnostic classification procedures are used in extracting diagnostic information[5], the diagnostic information contents (not to be confused with the signal information contents) of the standard 12-lead ECG and the VCG are practically identical[39].

The latter study appeared in 1987, when vectorcardiography had been discontinued at most clinical sites. One of the reasons for this discontinuation may have been the publication by Simonson *et al.*[40] in 1966. This research was done after several studies (summarized in the same publication[40]) had appeared that claimed superiority of vectorcardiography. Simonson and colleagues provided evidence for the conclusion that the diagnostic performance of experienced electrocardiographers was superior for the 12-lead ECG as compared to the VCG. Later, it became evident that automated diagnostic 12-lead ECG algorithms performed at

the level of the most accurate cardiologists[41], but for the VCG, statistical programs performed better than the cardiologists[42]. The diverse conclusions when comparing the diagnostic performance of the ECG to that of the VCG may, hence, well have been caused by the different evaluation methodology (visual inspection by an electrocardiographer versus automated diagnosis by a computer program). In practice, the standard 12-lead ECG remained the most popular variant and persisted, while the VCG vanished.

In the 1967 Recommendations for Standardization of Leads and of Specifications for Instruments in Electrocardiography and Vectorcardiography (see Figure 7), Kossmann and colleagues noted: "That there is redundant electrocardiographic information in the usually recorded 12 leads is generally agreed. However, when the suggestion is made to the clinician that the number of leads he is using now is excessive, resistance to change is encountered which results probably from the combination of long-ingrained habit and the inadequacy of clinicopathological and other correlations with orthogonal leads[36]". This observation was remarkably correct and routine clinical electrocardiography has continued to exist mainly in the form of the scalar 12-lead ECG.

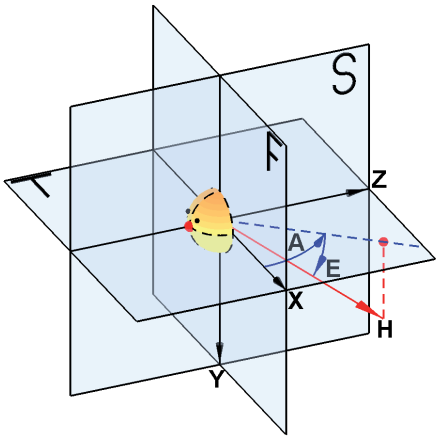

FIGURE 7. Pictorial summary of definitions of vectorcardiographic axes, planes and angles according to the AHA standardization recommendations[36]; Figure A1 from Man[43], with permission. X = vectorcardiographic x-axis (the arrow denotes the positive x direction); Y = y-axis; Z = z-axis; F = frontal plane; T = transverse plane; S = sagittal plane. As an example, an arbitrarily chosen instantaneous heart vector, H (red) is projected on the transverse plane (blue dotted line). The angle between the x-axis and this projection is the azimuth, A, of that heart vector (positive when turning in the direction of the positive z-axis). The angle between this projection and the heart vector is the elevation, E, of that heart vector (positive when turning in the direction of the positive y-axis). Hence, the heart vector as drawn in this Figure has a positive azimuth, a positive elevation, and positive amplitudes in the x-, y-, z directions.

Revival of vectorcardiography

With the decreasing clinical interest for vectorcardiography, attempts were made to mathematically synthesize, by matrix multiplication, a 12-lead ECG from a VCG, thus facilitating those who possessed VCG equipment to perform 12-lead ECG diagnosis, which has led to the development of the "Dower matrix"[44]. The interest in the diagnostic and prognostic value of the VCG has never completely subsided, however, and the past decades have shown a revival of the VCG. In retrospect, the turning point could be situated around 1987-1990 when there were three important publications about matrices for the mathematical synthesis of a Frank VCG from a 12-lead ECG recording — first by Levkov in 1987[45], then by Edenbrandt and Pahlm in 1988 (the "inverse Dower matrix")[46], and by Kors *et al.* in 1990[47] — thus facilitating those who possessed standard 12-lead ECG equipment to perform VCG diagnosis and research. This has led to what has been called "12-lead vectorcardiography"[48;49]. This made it possible to choose between or even combine 12-lead electrocardiographic and 3-lead vectorcardiographic computer analysis[50].

The matrix multiplication that synthesizes a VCG from a 12-lead ECG is algebraically noted as:

$$VCG = M \cdot ECG \qquad \text{(Eq. 2)}$$

where *VCG* is a matrix representation of the computed VCG samples, *ECG* a matrix representation of the originally recorded 12-lead ECG samples and *M* a matrix consisting of multiplication factors. This mathematical operation is illustrated in Figure 8; note that only 8 of the 12 ECG leads (I, II, V1-V6) are used because the remaining 4 extremity leads are fully redundant (can straightforwardly be computed from leads I and II and thus contain no independent information). Currently, the matrix by Kors and colleagues[47] is generally accepted as the best method to synthesize a VCG from a 12-lead ECG: "Kors is still most Frank"[51]. Figure 9 gives an example ECG recording and its synthesized VCG. Note how the Kors matrix coefficients as shown in Figure 8 determine the relative contribution of each original 8 ECG leads to each of the 3 synthesized VCG leads.

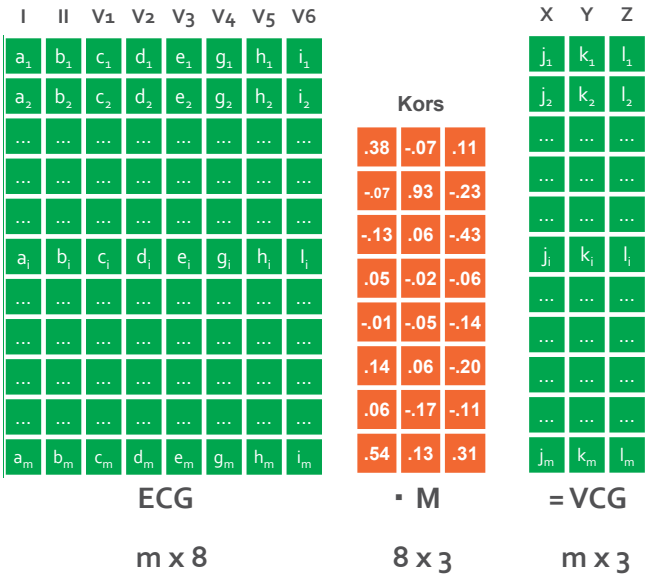

FIGURE 8. Illustration of the synthesis of a VCG from a 12-lead ECG by the Kors matrix. The originally measured electrocardiogram, mathematically synthesized vectorcardiogram and Kors weighting factors for this synthesis are represented by matrices ECG, VCG and M, respectively. The 12-lead electrocardiogram is represented by matrix ECG that has 8 columns; each of these columns a-i represents the ECG signal in one of the 8 independent leads I, II, V1-V6, respectively. The matrix has m rows, where m indicates the number of samples in the signal. Typically, in a routine clinical 10-s ECG sampled at 500 Hz, m = 5000. The synthesized vectorcardiogram is represented by matrix VCG that has 3 columns; each of these columns j-l represents one of the 3 orthonormal VCG leads X, Y and Z, respectively. The number of samples equals that of the electrocardiogram. The Kors matrix consists of 3 columns in each of which 8 multiplication factors are found to compute a weighted sum of the samples of the 8 ECG leads as follows (example for sample i):

– *Lead X*: $j_i = +.38 \cdot a_i - .07 \cdot b_i - .13 \cdot c_i \ldots + .54 \cdot i_i$
– *Lead Y*: $k_i = -.07 \cdot a_i + .93 \cdot b_i + .06 \cdot c_i \ldots + .13 \cdot i_i$
– *Lead Z*: $l_i = +.11 \cdot a_i - .23 \cdot b_i - .43 \cdot c_i \ldots + .31 \cdot i_i$

Unique vectorcardiography-bound information

Because the information in the 12-lead ECG is fairly redundant[36;52-54], reduction of the number of leads from eight (standard 12-lead ECG) to three (VCG) can be achieved with limited information loss[55]. Despite the fact that the VCG actually contains slightly less information than the ECG, VCG analysis/interpretation has additional value compared to ECG analysis/interpretation because the VCG gives access to information that remains unexplored in the standard 12-lead ECG. Examples of such unexplored information are:

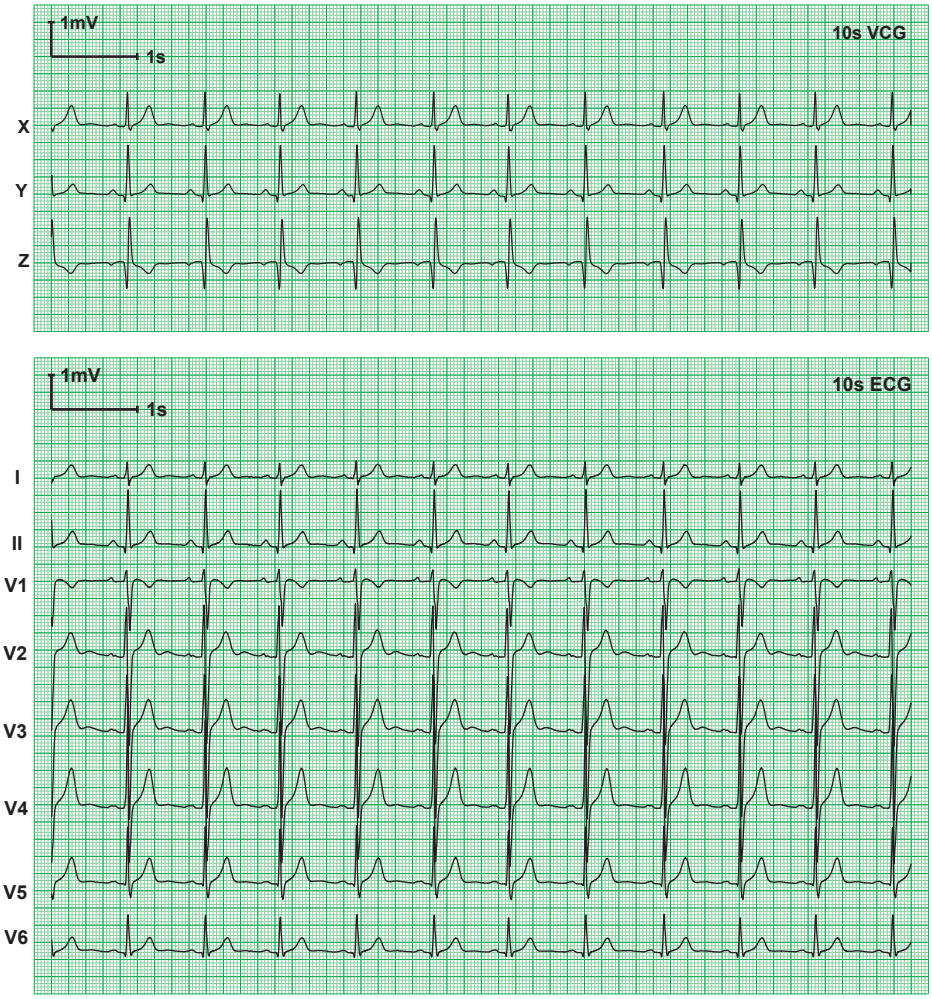

FIGURE 9. Example of a synthesized VCG (upper panel), computed from a standard 12-lead ECG (lower panel) by multiplication of the 8 independent ECG leads I, II, V1-V6 by the Kors matrix (see Figure 8 for the calculations). For an initial orientation it is useful to inspect the Kors matrix in Figure 8 to find the most important ECG leads that contribute to a given VCG lead. ECG leads V6 and I have major contributions to VCG lead X, with weighting factors of .54 and .38, respectively. ECG lead II has a major contribution to VCG lead Y, with a weighting factor of .93. ECG leads V1 and V6 have major contributions to VCG lead Z, with weighting factors of –.43 and .31, respectively (note that the ECG lead V1 weighting has a minus sign which means that the lead must be inverted). Visual comparison of lead X with leads V6 and I, of lead Y with lead II, of lead Z with inverted lead V1 and with lead V6 shows clear resemblance, however it has to be realized that each of the ECG leads contributes to each of the VCG leads and that the correctness (orthonormality) of the synthesized VCG actually requires the contributions by all ECG leads, also the smaller ones. Strikingly, in this example, the peak-peak amplitudes in the X, Y and Z leads have comparable magnitudes, while in the ECG the differences are large: *e.g.*, compare lead I to leads V3/V4; these differences are caused by the strongly different lead strengths in the electrocardiogram (see Figure 4).

- maximal amplitudes of the QRS complex and the T wave (as discussed above, and illustrated in Figure 5, in scalar electrocardiography every lead has its own sensitivity and its own timing of the maximum, while in spatial vectorcardiography there is only one calibrated maximal QRS- or T vector with a specific timing);
- QRS- and T-wave axes in three dimensions (instead of an approximated projection in the presumed frontal plane);
- spatial QRS- and T-wave integrals which are indexes for dispersion of depolarization and repolarization, respectively[56];
- spatial angle between the QRS- and T-wave axes which is a measure of concordance/discordance of the ECG[57] – see Figure 10;
- ventricular gradient (spatial QRS-T integral) which reflects the action potential morphology distribution in the heart[57] – the computation of the ventricular gradient is illustrated in Figure 11;
- ST vector (oftentimes measured at the J point or 40, 60 or 80 ms thereafter) which assesses ischemia, and is hence also called injury or ischemia vector;
- QRS- and T-loop complexity (healthy hearts have smooth planar loops; compromised hearts have irregular and distorted loops[58-61]).

Although they are not new, these vectorcardiographic variables have never played a significant role in clinical vectorcardiography as it was performed several

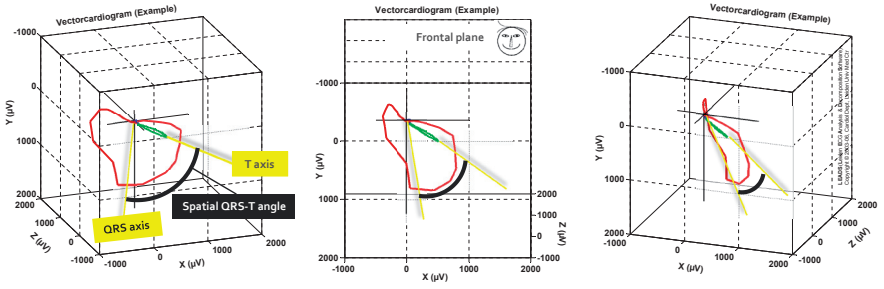

FIGURE 10. Illustration of the spatial QRS-T angle, normal subject (female, 20 years). The Figure shows the QRS- and the T loops (red and green, respectively; the T loop in this example is relatively narrow, as is often seen in normal subjects). The QRS- and T axes are the spatial orientations (azimuth and elevation) of the QRS- and T integrals (vectorial additions of the QRS- and T areas in the X, Y and Z leads, respectively). The three depicted views (from left to right: right-anterolateral, anterior and left-anterolateral) show clearly the influence of the projection: the "genuine" QRS-T angle in this subject, 81°, is best seen in the right-anterolateral view while the frontal view shows a QRS-T angle of only 43°. This demonstrates that the QRS-T angle should always be measured in 3D space and not in the frontal plane.

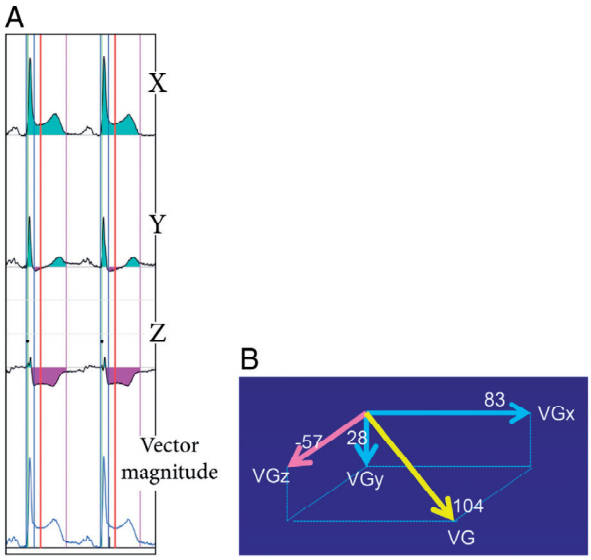

FIGURE 11. Illustration of the computation of the ventricular gradient (VG); Figure 2 from Ter Haar *et al.*[62], with permission. ECG of a patient with acute ischemia as a consequence of balloon occlusion of a coronary artery segment during elective percutaneous transluminal coronary angioplasty. Panel A: synthesized VCG (X, Y and Z leads) and vector magnitude. Vertical time markers indicate onset QRS, J point, J + 60-ms instant (red) and end of the T wave. The x, y, and z components of the VG vector are computed as the areas under the curve of the QRS-T complex; positive amplitudes (petrol) contribute positively and negative areas (purple) contribute negatively to the area. In this example, the net QRS-T areas of the X and the Y leads are obviously positive, while the net QRS-T area of the Z lead is negative. The latter is due to the ST depression and the negative T wave. Panel B: composition of the VG vector (vector sizes in mV·ms). The magnitudes of the x, y and z components, VG_x, VG_y and VG_z, equal the net QRS-T areas as illustrated in panel A. VG_x and VG_y are positive and point, hence, in the positive directions of the x- and the y axes. VG_z is negative and points, hence, in the negative direction of the z-axis. Vectorial summation of VG_x, VG_y and VG_z yields the resultant VG vector.

decades ago, although their potential has been recognized[63]. *E.g.*, Barker, in his book The Unipolar Electrocardiogram (1952)[64], wrote: "At the present time, the determination of the ventricular gradient is not a practical procedure for general use in electrocardiography. The theoretical foundation upon which it rests, however, are of utmost importance." All above mentioned variables are rather global VCG characteristics and have been explored to establish normal values, for diagnostic purposes and for risk stratification. These new descriptors of abnormality deserve to be further explored and exploited in future electrocardiography, not to replace the standard 12-lead electrocardiogram, but rather to enhance it.

Integration of 12-lead electrocardiography and vectorcardiography

With mathematically synthesized VCGs, it is feasible to add VCG analysis and interpretation ("12-lead vectorcardiography"[48;49]) to standard 12-lead ECG analysis and interpretation. This leaves the signal acquisition (electrodes, electronics) unaffected, and only requires appropriate additional software to process the ECG signal. Classical VCG diagnostic algorithms can be implemented and executed in addition to the current ECG diagnostic algorithms. This will likely increase diagnostic performance, as suggested by Macfarlane and Edenbrandt in 1992[65]. *E.g.*, Kors and colleagues reported that the MEANS ECG/VCG interpretation of the CSE database ECGs yielded a diagnostic accuracy of 69.8% for the ECG alone, a diagnostic accuracy of 70.5% for the synthesized VCG, and a diagnostic accuracy of 73.6% for the ECG and synthesized VCG in combination[66]. These figures, although impressive, still lag the performance of an expert panel of cardiologists by about 10%. Hence, there is room for further improvement of diagnostic accuracy. Such improvement could be achieved by utilizing the information in the synthesized VCG that remains unexplored in standard 12-lead ECG analysis. Specifically, so far incompletely explored information in the VCG (QRS integral, T-wave integral, QRS-T integral or ventricular gradient, and QRS-T angle) can help to generate new expertise regarding diagnostics and stratification. Together, this would help to bring clinical electrocardiography to a higher level, and such expectations are the major driving force for current VCG-oriented research.

Overview of thesis contents

This thesis consists of a number of chapters that have as a common denominator that they aim at a further incorporation of the VCG in clinical electrocardiography, by developing the necessary analysis algorithms, investigating methodology and by studying clinical data, with a focus on the ST injury vector in acute coronary syndrome, on the spatial QRS-T angle and on the ventricular gradient for diagnostic and prognostic purposes, and on vectorcardiographically-assessed T-wave alternans to predict serious ventricular arrhythmias in heart failure patients.

In **Chapter 2** a method is proposed to reconstruct standard 12-lead electrocardiograms from 12-lead electrocardiograms recorded with a Mason-Likar electrode

configuration (limb electrodes on the thorax instead of on wrists and ankles, usually applied in exercise electrocardiography and in monitoring conditions). Such a reconstruction is useful, because diagnostic ECG interpretation programs, *e.g.*, in electrocardiographs, have been developed on the basis of ECGs recorded with standard electrode positions. Reconstruction of the standard 12-lead ECG could, hence, improve diagnostics in Mason-Likar ECGs. After synthesizing VCGs from both standard 12-lead and Mason-Likar 12-lead ECGs, we studied how much vectorcardiographic features like the spatial QRS-T angle and the ventricular gradient differed. This would answer the question if reconstruction of a standard 12-lead ECG from a Mason-Likar ECG is needed prior to VCG synthesis for subsequent VCG analysis.

In **Chapter 3** a method is proposed to individually improve the ECG-to-VCG transformation quality. We have done this by comparing, intra-individually, the original ECG with a reconstructed ECG obtained by an inverse transformation of the synthesized VCG. We implemented the errors-in-variables method to reduce, intra-individually, the difference between the original and the reconstructed ECG at the cost of an "error" in the ECG-to-VCG transformation matrix. This "error" in the transformation matrix is in fact an adaptation towards an individualized ECG-to-VCG transformation matrix that is expected to perform better than a "one-size-fits-all" matrix.

In **Chapter 4** a program is described that we have developed in our department to perform a beat-to-beat vectorcardiographic analysis of dynamic ECGs, *e.g.*, recorded during exercise tests. This facilitates, amongst others, vectorcardiographic T-wave alternans analysis as used in other studies that are described in this thesis.

Chapter 5 describes the size and direction of the ST injury vector as measured in a group of patients with acute coronary syndrome and a totally occluded culprit artery. One question to investigate was how many of the patients had ST-elevation and non-ST-elevation ECGs and how this would relate to and be explained by the vectorcardiographically computed ST injury vector.

Chapter 6 compares the spatial QRS-T angles computed from VCGs that are synthesized from ECGs by either the inverse Dower ECG-to-VCG transformation matrix[46] or the Kors ECG-to-VCG transformation matrix[47]. Both matrices are popular. The inverse Dower matrix was the first attempt to synthesize a VCG from a 12-lead ECG and was based on the Frank torso model. The Kors matrix is a statistical optimization to fit synthesized VCGs with actually recorded Frank VCGs in a patient population in whom simultaneously 12-lead ECGs and Frank VCGs were recorded. Currently, the Kors matrix is considered superior to the inverse Dower matrix. It is important to study the differences between the inverse Dower and Kors QRS-T angles, because several older QRS-T studies were done with VCGs synthesized by the inverse Dower matrix and the question is if the results of these older studies remain valid in the "Kors era".

Chapter 7 describes the consequences of the choice for a given vectorcardiogram synthesis matrix (inverse Dower[46] vs. Kors[47]) on the power of the electrocardiogram-derived spatial QRS-T angle to predict arrhythmias in patients with ischemic heart disease and systolic left ventricular dysfunction.

In **Chapter 8** the role of the spatial QRS-T angle in diagnosing left ventricular hypertrophy was investigated. We performed this study in a group of patients with an ECG interpretation of either normal or left ventricular hypertrophy in all of whom echocardiograms had been made that were diagnosed as either normal or as having left ventricular hypertrophy.
T-wave alternans is used as a noninvasive index for the occurrence of serious ventricular arrhythmias in heart failure patients. As such it is sometimes used as an extra criterion for the decision to implant a cardioverter-defibrillator or not.

In **Chapter 9** we ranked, in an ECG database of mixed cardiovascular pathology and healthy subjects, the synthesized VCGs on two different measures of T-wave alternans: T-wave integral and maximal T-wave vector. Currently, T-wave alternans is usually measured as alternans in the maximal T-wave amplitude. Purpose of our study was to see whether alternans in a vectorcardiographic feature, namely the T-wave integral would show a similar ranking as the more conventional T-wave amplitude.

Chapter 10 reports about the predictive power of T-wave alternans and of the ventricular gradient hysteresis for the occurrence of serious ventricular arrhythmias in a group patients who had an implanted cardioverter-defibrillator for primary prevention of serious ventricular arrhythmias.
In **Chapter 11** we studied the predictive power of T-wave alternans for serious ventricular arrhythmias in heart failure patients who had an implanted cardioverter-defibrillator for reasons of primary prevention. Usually, T-wave alternans is measured in exercise ECGs, because exercise increases the T-wave alternans amplitude. This increase is seen in patients and in normals, and cannot be taken as the proof that exercise is needed to measure T-wave alternans for predictive purposes. For this reason, we have compared the predictive value of T-wave alternans measured during exercise with several vectorcardiographic features in the resting ECGs of the same patients.

Chapter 12, finally, compares standard and vectorcardiographic leads for the purpose of repolarization alternans identification.

References

1. Braunwald E. The rise of cardiovascular medicine. *Eur Heart J* 2012;33:838-846.
2. Macfarlane PW, Van Oosterom A, Pahlm O, Kligfield P, Janse M, Camm J. *Comprehensive electrocardiology*. Second ed. London: Springer-Verlag, 2011.
3. Waller AD. A demonstration on man of electromotive changes accompanying the heart's beat. *J Physiol* 1887;8:229-234.
4. Rautaharju PM. A hundred years of progress in electrocardiography. 1: Early contributions from Waller to Wilson. *Can J Cardiol* 1987;3:362-374.
5. Rautaharju PM. A hundred years of progress in electrocardiography. 2: The rise and decline of vectorcardiography. *Can J Cardiol* 1988;4:60-71.
6. Einthoven W, Fahr G, de Waart A. Über die Richtung und die manifeste Grösse der Potentialschwankungen im menschlichen Herzen und über den Einfluss der Herzlage auf die Form des Elektrokardiogramms. *Pflüger Arch ges Physiol* 1913;150:275-315.
7. Einthoven W, Fahr G, de Waart A. On the direction and manifest size of the variations of potential in the human heart and on the influence of the position of the heart on the form of the electrocardiogram. *Am Heart J* 1950;40:163-211.
8. Barnes AR, Pardee HEB, White PD, Wilson FN, Wolferth CC. Standardization of precordial leads: Supplementary report. *Am Heart J* 1938;15:235-239.
9. Standardization of precordial leads: Joint recommendations of the American Heart Association and the Cardiac Society of Great Britain and Ireland. *Am Heart J* 1938;15:107-108.
10. Standardisation of precordial leads: Joint recommendations of the Cardiac Society of Great Britain and Ireland and the American Heart Association. *The Lancet* 1938;231:221-222.
11. Goldberger E. A simple, indifferent, electrocardiographic electrode of zero potential and a technique of obtaining augmented, unipolar, extremity leads. *Am Heart J* 1942;23:483-492.
12. Wilson FN, Johnston FD, Macleod AG, Barker PS. Electrocardiograms that represent the potential variantions of a single electrode. *Am Heart J* 1934;9:447-458.
13. Wolferth CC, Wood CW. The electrocardiographic diagnosis of coronary occlusion by the use of chest leads. *Am J Med Sci* 1932;183:30-34.
14. Mason RE, Likar I. A new system of multiple-lead exercise electrocardiography. *Am Heart J* 1966;71:196-205.
15. Man SC, Maan AC, Kim E, Draisma HH, Schalij MJ, van der Wall EE *et al.* Reconstruction of standard 12-lead electrocardiograms from 12-lead electrocardiograms recorded with the Mason-Likar electrode configuration. *J Electrocardiol* 2008;41:211-219.
16. Waller AD. Introductory address on the electromotive properties of the human heart. *Br Med J* 1888;2:751-754.
17. Waller AD. On the electromotive changes connected with the beat of the mammalian heart, and of the human heart in particular. *Phil Trans R Soc Lond B* 1889;180:169-194.

18. Malmivuo J, Plonsey R. Vectorcardiographic lead systems. In: Malmivuo J, Plonsey R, eds. *Bioelectromagnetism. Principles and applications of bioelectric and biomagnetic fields*. New York, Oxford: Oxford University Press; 1995:290-306.
19. Van Herpen G. Professor Herman Burger (1893-1965), eminent teacher and scientist, who laid the theoretical foundations of vectorcardiography - and electrocardiography. *J Electrocardiol* 2014;47:168-174.
20. Burger HC, Van Milaan JB. Heart-vector and leads; geometrical representation. *Br Heart J* 1948;10:229-233.
21. Burger HC, van Brummelen A, Van Herpen G. Heartvector and leads. *Am Heart J* 1961;61:317-323.
22. Boutkan J. *Vectorcardiography: physical bases and clinical practice*. First ed. Eindhoven: Centrex Publishing Company, 1965.
23. Malmivuo J, Plonsey R. Theoretical methods for analyzing volume sources and volume conductors. In: Malmivuo J, Plonsey R, eds. *Bioelectromagnetism. Principles and applications of bioelectric and biomagnetic fields*. New York, Oxford: Oxford University Press; 1995:185-226.
24. Malmivuo J, Plonsey R. Summary of the ECG lead systems. In: Malmivuo J, Plonsey R, eds. *Bioelectromagnetism. Principles and applications of bioelectric and biomagnetic fields*. New York, Oxford: Oxford University Press; 1995:309-312.
25. Malmivuo J, Plonsey R. Distortion factors in the ECG. In: Malmivuo J, Plonsey R, eds. *Bioelectromagnetism. Principles and applications of bioelectric and biomagnetic fields*. New York, Oxford: Oxford University Press; 1995:313-319.
26. Williams HB. On the cause of the phase difference frequently observed between homnymous peaks of the electrocardiogram. *Am J Physiol* 1914;35:292-300.
27. Wilson FN, Johnston FD. The vectorcardiogram. *Am Heart J* 1938;16:14-28.
28. Schellong F. Elektrokardiographische Diagnostik der Herzmuskelerkrankungen. *Verhandl d deutch Gesellsch f inn Med* 1936;48:288.
29. Mann H. A method of analyzing the electrocardiogram. *Arch Intern Med* 1920;25:83-94.
30. McFee R, Parungao A. An orthogonal lead system for clinical electrocardiography. *Am Heart J* 1961;62:93-100.
31. Schmitt OH, Simonson E. Symposium on electrocardiography and vectorcardiography: the present status of vectorcardiography. *AMA Arch Intern Med* 1955;96:574-590.
32. Frank E. An accurate, clinically practical system for spatial vectorcardiography. *Circulation* 1956;13:737-749.
33. Frohlich ED. Robert P. Grant, MD. *Am J Cardiol* 2003;91:646-648.
34. Silverman ME. J. Willis Hurst--a man of achievement. *Clin Cardiol* 1997;20:584-586.
35. Burch GE, DePasquale NP. *A history of electrocardiography*. 1st ed. Chicago: Year Book Medical Publishers, 1964.
36. Kossman CE, Brody DA, Burch GE, Hecht HH, Johnston FD, Kay C *et al.* Report of committee on electrocardiography, American Heart Association. Recommendations for standardization of leads and of specifications for instruments in electrocardiography and vectorcardiography. *Circulation* 1967;35:583-602.

37. Frank E. The image surface of a homogeneous torso. *Am Heart J* 1954;47:757-768.
38. Von der Groeben J. Decision rules in electrocardiography and vectorcardiography. *Circulation* 1967;36:136-147.
39. Willems JL, Lesaffre E, Pardaens J. Comparison of the classification ability of the electrocardiogram and vectorcardiogram. *Am J Cardiol* 1987;59:119-124.
40. Simonson E, Tuna N, Okamoto N, Toshima H. Diagnostic accuracy of vectorcardiogram and electrocardiogram - A cooperative study. *American Journal of Cardiology* 1966;17:829-878.
41. Willems JL, Abreu-Lima C, Arnaud P, van Bemmel JH, Brohet C, Degani R *et al.* The diagnostic performance of computer programs for the interpretation of electrocardiograms. *N Engl J Med* 1991;325:1767-1773.
42. Corabian, P. Accuracy and reliability of using computerized interpretation of electrocardiograms for routine examinations. Alberta, Canada. Alberta Heritage Foundation for Medical Research 2002;14.
43. Man S, Rahmattulla C, Maan AC, van der Putten NH, Dijk WA, van Zwet EW *et al.* Acute coronary syndrome with a totally occluded culprit artery: relation of the ST injury vector with ST-elevation and non-ST elevation ECGs. *J Electrocardiol* 2014;47:183-190.
44. Dower GE, Machado HB, Osborne JA. On deriving the electrocardiogram from vectorcardiographic leads. *Clin Cardiol* 1980;3:87-95.
45. Levkov CL. Orthogonal electrocardiogram derived from the limb and chest electrodes of the conventional 12-lead system. *Med Biol Eng Comput* 1987;25:155-164.
46. Edenbrandt L, Pahlm O. Vectorcardiogram synthesized from a 12-lead ECG: superiority of the inverse Dower matrix. *J Electrocardiol* 1988;21:361-367.
47. Kors JA, Van Herpen G, Sittig AC, van Bemmel JH. Reconstruction of the Frank vectorcardiogram from standard electrocardiographic leads: diagnostic comparison of different methods. *Eur Heart J* 1990;11:1083-1092.
48. Macfarlane PW. Derived vectorcardiogram - 12 lead vectorcardiography. In: Macfarlane PW, Van Oosterom A, Pahlm O, Kligfield P, Janse M, Camm J, eds. *Comprehensive Electrocardiology*. Second ed. London: Springer-Verlag; 2011:404-405.
49. Macfarlane PW, Pahlm O. 12 lead vectorcardiography. In: Macfarlane PW, Van Oosterom A, Pahlm O, Kligfield P, Janse M, Camm J, eds. *Comprehensive Electrocardiology*. Second ed. London: Springer-Verlag; 2011:1951-2006.
50. Kors JA, Van Herpen G. Computer analysis of the electrocardiogram. In: Macfarlane PW, Van Oosterom A, Pahlm O, Kligfield P, Janse M, Camm J, eds. *Comprehensive Electrocardiology*. Second ed. London: Springer-Verlag; 2011:1723-1756.
51. Cortez D, Sharma N, Devers C, Devers E, Schlegel TT. Visual transform applications for estimating the spatial QRS-T angle from the conventional 12-lead ECG: Kors is still most Frank. *J Electrocardiol* 2014;47:12-19.
52. Dower GE, Yakush A, Nazzal SB, Jutzy RV, Ruiz CE. Deriving the 12-lead electrocardiogram from four (EASI) electrodes. *J Electrocardiol* 1988;21(Suppl):182-187.
53. Kors JA, van HG. How many electrodes and where? A "poldermodel" for electrocardiography. *J Electrocardiol* 2002;35(Suppl):7-12.

54. Nelwan SP, Kors JA, Meij SH. Minimal lead sets for reconstruction of 12-lead electrocardiograms. *J Electrocardiol* 2000;33(Suppl):163-166.
55. Augustyniak P. On the equivalence of the 12-Lead ECG and the VCG representations of the cardiac electrical activity. 10th International conference on system modelling control; Zakopane 2001:51-56.
56. Van Oosterom A. Reflections on the T waves. Advances in Electrocardiology; Singapore 2005:807-815.
57. Draisma HH, Schalij MJ, van der Wall EE, Swenne CA. Elucidation of the spatial ventricular gradient and its link with dispersion of repolarization. *Heart Rhythm* 2006;3:1092-1099.
58. De Ambroggi L, Aime E, Ceriotti C, Rovida M, Negroni S. Mapping of ventricular repolarization potentials in patients with arrhythmogenic right ventricular dysplasia: principal component analysis of the ST-T waves. *Circulation* 1997;96:4314-4318.
59. Perkiomaki JS, Hyytinen-Oinas M, Karsikas M, Seppanen T, Hnatkova K, Malik M *et al.* Usefulness of T-wave loop and QRS complex loop to predict mortality after acute myocardial infarction. *Am J Cardiol* 2006;97:353-360.
60. Priori SG, Mortara DW, Napolitano C, Diehl L, Paganini V, Cantu F *et al.* Evaluation of the spatial aspects of T-wave complexity in the long-QT syndrome. *Circulation* 1997;96:3006-3012.
61. Zabel M, Malik M, Hnatkova K, Papademetriou V, Pittaras A, Fletcher RD *et al.* Analysis of T-wave morphology from the 12-lead electrocardiogram for prediction of long-term prognosis in male US veterans. *Circulation* 2002;105:1066-1070.
62. Ter Haar CC, Maan AC, Warren SG, Ringborn M, Horacek BM, Schalij MJ *et al.* Difference vectors to describe dynamics of the ST segment and the ventricular gradient in acute ischemia. *J Electrocardiol* 2013;46:302-311.
63. Hurst JW. Thoughts about the ventricular gradient and its current clinical use (Part I of II). *Clin Cardiol* 2005;28:175-180.
64. Barker JM. *The unipolar electrocardiogram: A clinical interpretation*. First ed. New York: Appleton-Century-Crofts, 1952.
65. Macfarlane PW, Edenbrandt L. 12-lead vectorcardiography in ischemic heart disease. *J Electrocardiol* 1992;24(Suppl):188-193.
66. Kors JA, van HG, Willems JL, van Bemmel JH. Improvement of automated electrocardiographic diagnosis by combination of computer interpretations of the electrocardiogram and vectorcardiogram. *Am J Cardiol* 1992;70:96-99.